Article

Not peer-reviewed version

Synergistic Oncolytic Effect of HSVtk- and IL-15Rα-Armed Vaccinia Viruses Inducing Systemic Antitumor Immunity

Olga N. Alekseeva *, Pavel O. Vorobyev *, Yasmin Shakiba, Stepan A. Ionov, Svetlana S. Antseva, Anastasia Semenova, Marat P. Valikhov, Vladimir A. Kalsin, Veronika V. Vadekhina, Dmitry V. Kochetkov, Peter M. Chumakov, Anastasia V. Poteryakhina

Posted Date: 14 May 2026

doi: 10.20944/preprints202605.0960.v1

Keywords: vaccinia virus; ganciclovir

Article

Synergistic Oncolytic Effect of HSVtk - and IL-15Rα-Armed Vaccinia Viruses Inducing Systemic Antitumor Immunity

Olga N. Alekseeva [1,*], Pavel O. Vorobyev [1,*], Yasmin Shakiba [1], Stepan A. Ionov [1,2], Svetlana S. Antseva [1], Anastasia Semenova [1], Marat P. Valikhov [1], Vladimir A. Kalsin [3], Veronika V. Vadekhina [4], Dmitry V. Kochetkov [1], Peter M. Chumakov [1] and Anastasia V. Poteryakhina [1]

[1] Engelhard Institute of Molecular Biology, Russian Academy of Science, 119991, Moscow, Russia
[2] Moscow Center for Advanced Studies, Kulakova Str. 20, 123592, Moscow, Russia
[3] Federal Scientific and Clinical Center for Specialized Types of Medical Care and Medical Technologies, Federal Medical and Biological Agency, 115682, Moscow, Russia
[4] Serbsky National Medical Research Center for Psychiatry and Narcology, Ministry of Health of the Russian Federation, 119034, Moscow, Russia
* Correspondence: olga_aleks@eimb.ru (O.N.A); pavel.gealbhain@gmail.com (P.O.V)

Abstract

Oncolytic virotherapy offers a promising avenue for solid tumor treatment, yet single-agent approaches are frequently limited by insufficient tumor lysis and inadequate immune activation. Here we report that combined therapy with two recombinant variants of the oncolytic vaccinia virus, armed with either herpes simplex virus thymidine kinase (VV-HSVtk) or the interleukin 15 receptor subunit alpha (VV-mIL15Rα), induces enhanced cytotoxicity and immune stimulation in a murine mammary adenocarcinoma model (4T1). In vitro, VV-HSVtk exhibited dose-dependent cytotoxicity markedly potentiated by ganciclovir (GCV) through HSVtk-mediated phosphorylation into a cytotoxic nucleoside analogue, and co-culture of VV-infected tumor cells with donor-derived NK cells further amplified oncolytic efficiency. In vivo, combined treatment with VV-HSVtk, VV-mIL15Rα, and GCV resulted in significant tumor regression and extended survival relative to monotherapy controls in 4T1 syngeneic mice. Histological examination revealed robust lymphocytic infiltration at tumor sites and absence of hepatic or splenic toxicity. Mechanistically, VV-mIL15Rα-driven IL-15 trans-presentation amplified immune cell activation, while VV-HSVtk/GCV provided targeted tumor debulking and immunogenic cell death, collectively reshaping the immunosuppressive tumor microenvironment. These findings establish a multimodal oncolytic platform combining direct viral cytotoxicity, suicide gene therapy, and cytokine-mediated immune co-stimulation as a translatable strategy for treating solid tumors.

Keywords: vaccinia virus; ganciclovir

1. Introduction

Oncolytic virus (OV) therapy has emerged as a transformative modality in precision oncology, utilizing viruses that selectively replicate within and lyse malignant cells while sparing healthy tissues [1,2]. Beyond direct oncolysis, OVs function as potent immunostimulatory agents capable of reversing the immunosuppressive tumor microenvironment (TME) and priming systemic anti-cancer immunity [3]. This therapeutic potential is exemplified by T-VEC, a GM-CSF-encoding herpes simplex virus and the first FDA-approved OV for melanoma [4]. Among the various viral platforms, vaccinia viruses (VVs) are particularly advantageous due to their significant transgene-encoding capacity, robust safety profile, and natural tropism for neoplastic tissues [5].

 doi:10.20944/preprints202605.0960.v1

A primary approach to enhance VV potency involves integrating immunostimulatory transgenes, like cytokines, to connect direct oncolysis with broad systemic antitumor immunity [6,7]. Interleukin-15 (IL-15) is a pleiotropic cytokine essential for the development, activation, and survival of cytotoxic T cells and natural killer (NK) cells [8]. Its biological activity is dramatically enhanced when complexed with the interleukin-15 receptor subunit alpha (IL-15Rα), which mediates high-affinity signaling and promotes long-term lymphoid survival [9]. Recent studies have demonstrated that VVs encoding IL-15 or IL-15/IL-15Rα fusion proteins can induce remission in various cancer models, particularly when combined with checkpoint inhibitors [10,11].

In addition to immunotherapy, metabolic "suicide gene" therapy (such as herpes simplex virus thymidine kinase - HSVtk system) offers a powerful method to enhance local tumor destruction [12,13]. When combined with the prodrug ganciclovir (GCV), HSVtk converts the drug into a cytotoxic triphosphate form that inhibits DNA synthesis [14]. This system is characterized by a "bystander effect," where the toxic metabolites spread to neighboring non-containing HSVtk tumor cells, significantly amplifying viral oncolytic footprint [15].

In this study, we utilized the Lister strain of vaccinia virus from the Institute of Viral Preparation (LIVP), an attenuated variant with established efficacy for treatment of highly immunosuppressive models like triple-negative breast cancer (TNBC) [16,17]. We engineered two recombinant variants: VV-HSVtk and VV-mIL15ra with a disrupted thymidine kinase gene and RFP expression within a bicistronic cassette [11].

In the present study, we investigated whether the combined use of a metabolically armed HSVtk-expressing LIVP variant and an immunostimulatory mIL-15Rα-expressing LIVP variant, together with ganciclovir, could improve local tumor destruction and enhance systemic antitumor immune responses. The therapeutic efficacy of this multimodal approach was assessed in vitro across murine and human tumor cell models and in vivo in the syngeneic 4T1 breast carcinoma model.

2. Results

2.1. Construction and Characterization of Recombinant LIVP Variants

The recombinant vaccinia virus variants were engineered via homologous recombination, targeting the viral thymidine kinase (TK) locus to enhance tumor selectivity [5]. The reporter gene tagRFP was utilized for visualization of viral replication and efficacy of transgene expression (Figure 1A). Successful integration of expression cassettes into the LIVP genome was confirmed by Sanger sequencing of the amplified TK locus.

 doi:10.20944/preprints202605.0960.v1

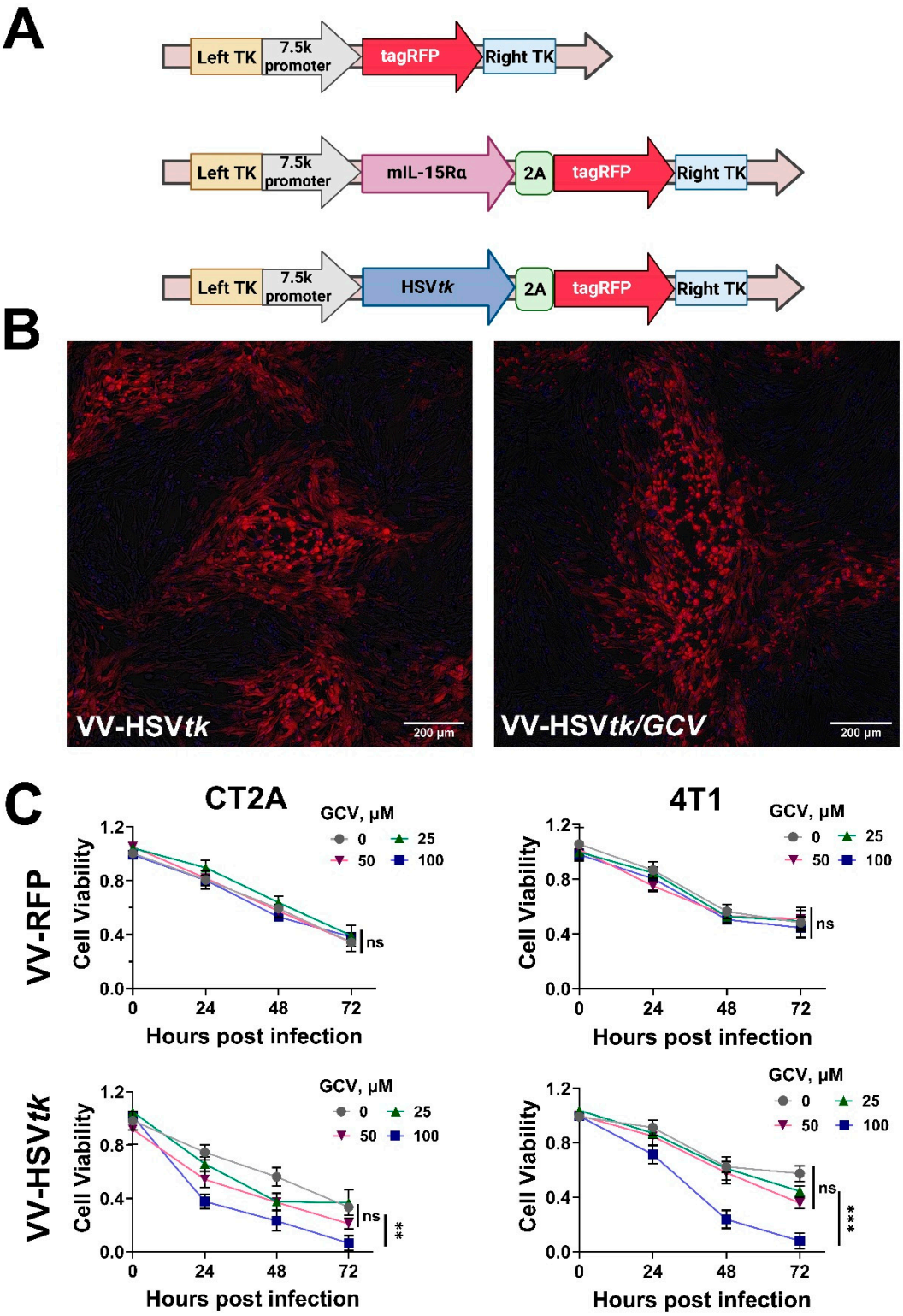

Figure 1. (a) Scheme of genetic modification of TK gene locus; (b) Microphotographs of viral plaques on BHK21 cells; (c) Comparison of cytotoxic effect of VV-RFP and VV-HSVtk strains in presence of ganciclovir (GCV) in the range of concentrations on CT2A and 4T1 cell lines at MOI=10. Statistical analysis was performed using the Mann-Whitney U-test or the log-rank test, * $p<0.05$, ** $p< 0.01$, *** $p< 0.001$, **** $p< 0.0001$.

Infectivity and cytolytic effect of the variants was dynamically assessed on BHK-21, CT2A and 4T1 cells (Figure S1). Fluorescence microscopy confirmed that both VV-HSVtk and VV-mIL15ra effectively infected and replicated within these cell lines (Figures 1B and 1C). RT-PCR confirmed

 doi:10.20944/preprints202605.0960.v1

robust expression of HSV1 thymidine kinase in lysates from VV-HSVtk-RFP-infected cells, laying the groundwork for ganciclovir-induced cytotoxicity (Figure S2). Kinetic properties of VV-mIL15Ra variant were described in detail earlier [11].

2.2. LIVP Recombinant Strains Demonstrate Enhanced Oncolysis via Metabolic Cooperation and NK Cell Recruitment

Treating immunologically "cold" tumors remains a formidable challenge in oncology due to a hostile tumor microenvironment (TME) characterized by poor infiltration of effector cells and a lack of inflammatory signaling. To address this, we engineered an oncolytic platform designed to "heat up" these non-immunogenic environments through a multi-modal attack [18]. We performed an assessment of its efficacy across a diverse panel of human cancer cell lines, tracking cytotoxicity at 24-, 48-, 72-, and 96-hours post-infection. The integration of the VV-HSVtk strain, when combined with GCV, catalyzed a profound dose-dependent escalation in cytotoxicity that effectively surpassed the baseline oncolytic activity of the VV-RFP variant. As observed at GCV concentration of 100 μM, cell viability was drastically compromised, validating the successful activation of a potent bystander effect. This allows toxic molecules to diffuse through gap junctions to eliminate adjacent uninfected cells, effectively circumventing the barriers to viral spread often found in dense immunosuppressive tumors [19].

Beyond direct metabolic lysis, our aim is to reprogram the TME to favor innate immune engagement. By co-culturing human cancer lines—including HeLa, HEK293T, HCT116, NCI-H460, TOV21G, DU145, MCF7, and C33A—with primary human Natural Killer (NK) cells, we observed that the presence of these effector cells significantly accelerated the destruction of cells infected with VV-HSVtk.

To further assess whether viral infection could facilitate innate immune-mediated tumor destruction, infected cultures were co-incubated with donor-derived human NK cells (Figure 2A-B). The presence of NK cells significantly enhanced the elimination of VV-HSVtk-infected tumor cells compared with virus treatment alone, whereas this effect was less pronounced in control samples, infected with VV-RFP. These findings indicate that metabolic cytotoxicity induced by HSVtk/GCV can be further complemented by immune effector cell activity. This transformation of the "cold" tumor landscape into a pro-inflammatory site facilitates the recruitment and activation of NK cells, providing a robust strategy for overcoming the inherent resistance of immunosuppressive malignancies [20].

Preprints.org (www.preprints.org) | NOT PEER-REVIEWED | Posted: 14 May 2026 doi:10.20944/preprints202605.0960.v1

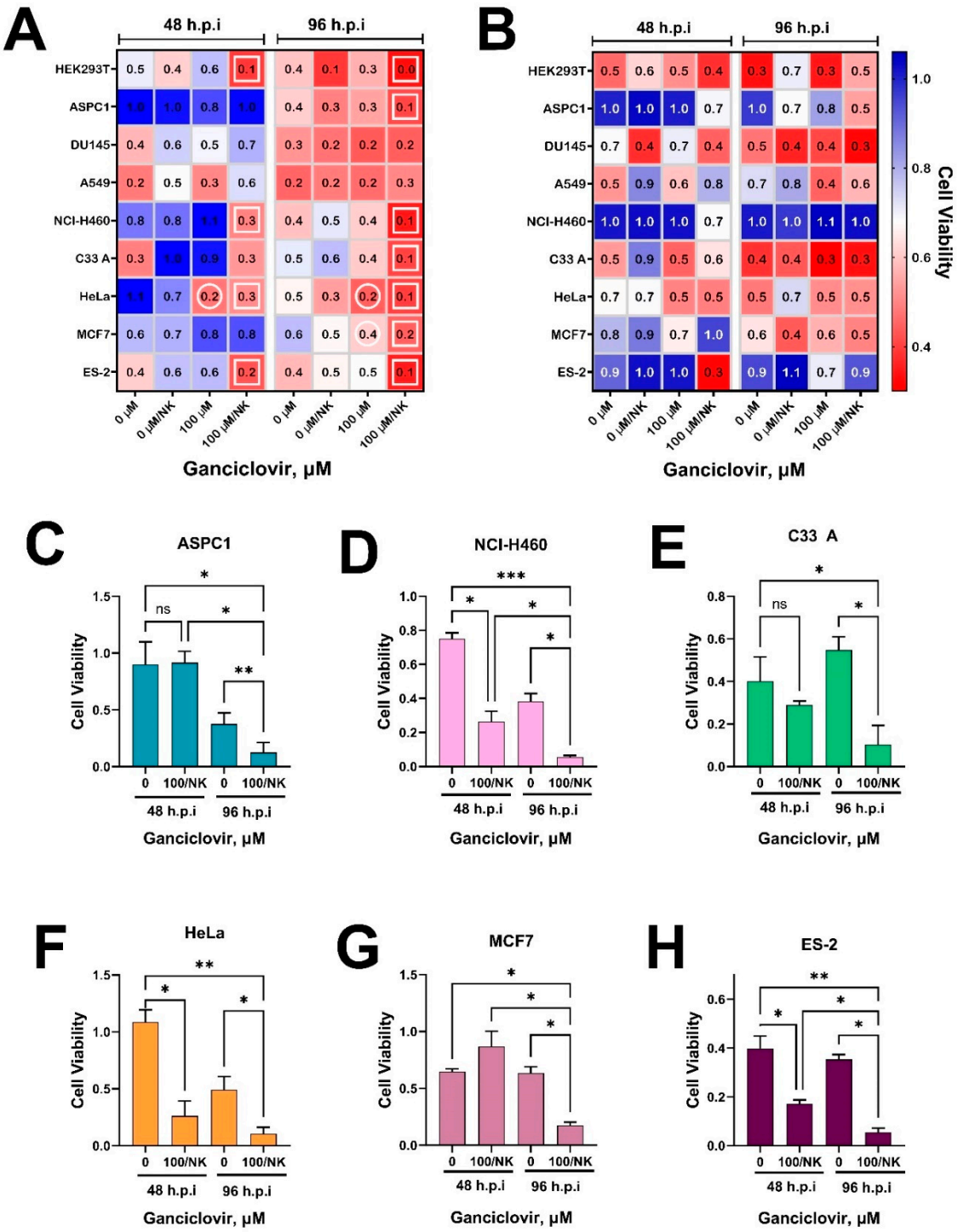

Figure 2. (a) Heatmap of cell viability after infection of VV-HSVtk at 48 and 96 hours post infection. Combined treatment included addition of GCV in concentration of 100 μm and donor human natural killer (NK) cells. Circles indicate statistically significant differences between replicates with or without GCV, squares - in presence or absence of NK cells. (b) Heatmap of cell viability after infection with control strain VV-RFP. (c)-(h) Comprehensive comparison of cell viability in different model cell lines treated with or without adding a combination of GCV and NK cells after 48 and 96 h.p.i. Statistical analysis was performed using the two-way ANOVA, * $p<0.05$, ** $p< 0.01$, *** $p< 0.001$.

 doi:10.20944/preprints202605.0960.v1

2.3. Combined Therapy with VV-HSVtk, VV-mIL15Ra and Ganciclovir Induces Synergistic Tumor Regression In Vivo

To evaluate the therapeutic potential of the recombinant strains, syngeneic mice bearing 4T1 breast carcinoma were treated with virotherapeutic agents alone or in combinationonce tumors reached a volume of approximately 50 mm³. The treatment regimen consisted of five intratumoral injections administered every four days. In groups receiving Ganciclovir (GCV), the prodrug was administered 48 hours following each viral injection to allow for sufficient expression of theHSVtk transgene. Tumor growth kinetics revealed that all viral treatment groups experienced reduced tumor progression compared to the Saline and GCV-only control groups. While monotherapies with VV-HSVtk or VV-mIL15Ra showed moderate inhibitory effects, the addition of GCV to the VV-HSVtk group significantly enhanced local tumor debulking, confirming the in vivo efficacy of the metabolic suicide gene system. Notably, the VV-mIL15Rα/GCV group did not show significant improvement over VV-mIL15Ra alone, as expected given the absence of the prodrug converting transgene.

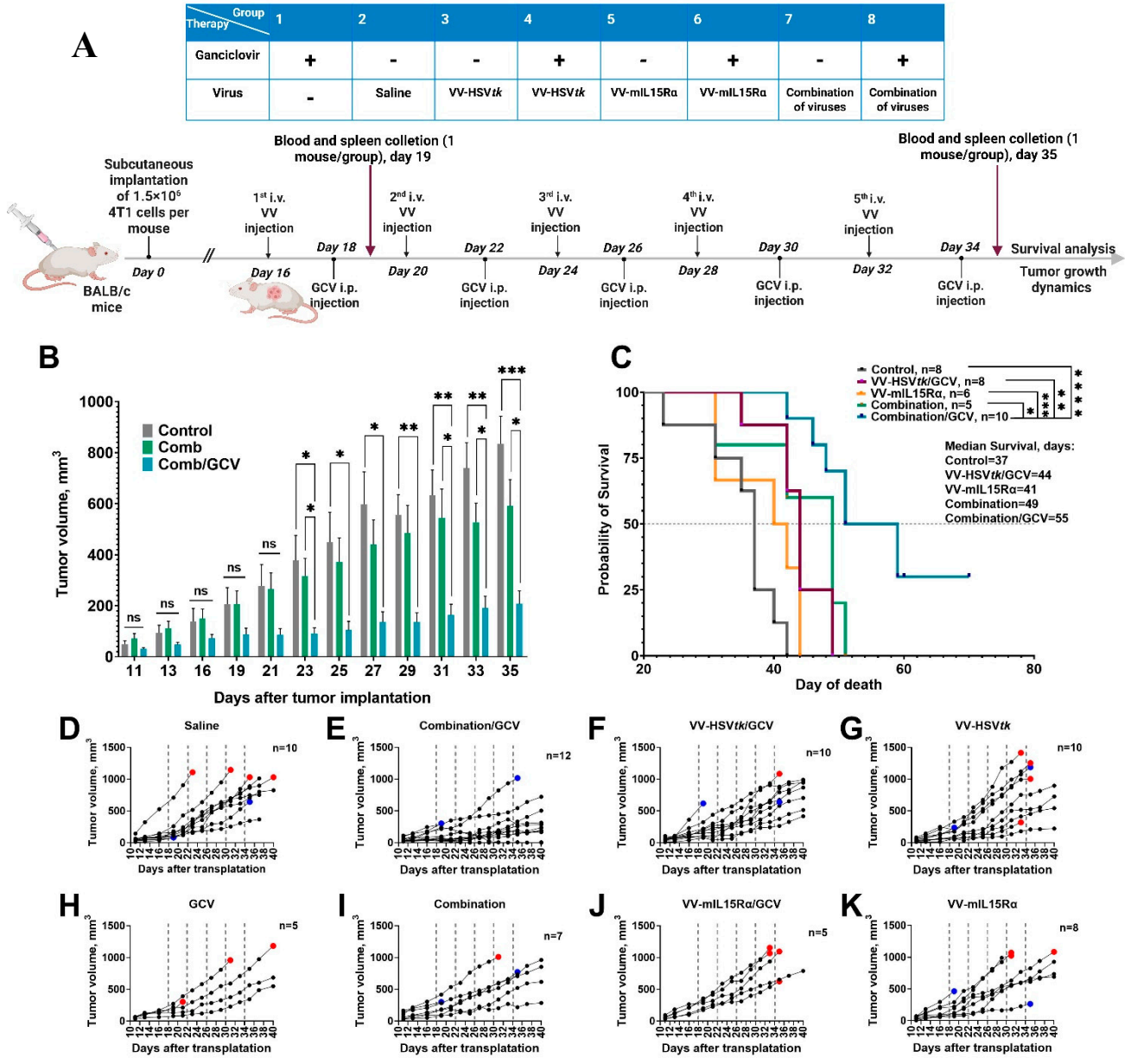

Figure 3. (a) Scheme of in vivo experiment; (b) Dynamic of tumor growth (c) Kaplan-Meier survival curves; (d)-(k) Tumor volume growth curves for individual mice in each treatment group (d)-control group, (e)- VV- HSVtk

 doi:10.20944/preprints202605.0960.v1

+VV- IL15Ra +GCV, (f)- VV-HSVtk+GCV, (g)-VV- HSVtk, (h) – GCV, (i)- VV- HSVtk +VV- IL15Ra, (j) - VV-IL15Ra + GCV, (k) - VV- IL15Ra. Statistical analysis was performed using the Mann-Whitney U-test or the log-rank test, * $p<0.05$, ** $p< 0.01$, *** $p< 0.001$, **** $p< 0.0001$.

The strongest therapeutic effect was observed in the triple combination group receiving VV-HSVtk, VV-mIL-15Rα and GCV, showing the slowest tumor progression, the highest frequency of complete tumor regression, and the longest median survival among all treatment groups. In contrast, monotherapy and dual-treatment groups produced only partial growth inhibition. These findings suggest that HSVtk/GCV-mediated metabolic cytotoxicity and mIL-15Rα-associated immune stimulation act cooperatively to improve tumor control in the highly aggressive 4T1 breast carcinoma model. Notably, 35% of mice in the combination therapy group demonstrated durable tumor growth arrest, with sustained suppression of tumor progression observed throughout the 70-day follow-up period; remarkably, one animal exhibited complete tumor regression, suggesting the induction of a curative antitumor immune response in a subset of treated subjects. It's particularly notable as 4T1 is widely regarded as one of the most immunosuppressive and treatment resistant preclinical breast cancer mode, characterized with profound CD8+ T cell exclusion and exhaustion [21].

2.4. Systemic Immune Activation: Enhanced T Cell Function

FluoroSpot analysis of IFN-γ- and IL-2-secreting T cells in PBMC revealed transient decrease in the number of antigen-specific T cells across all virus-treated groups following the first injection (Figure 4D). This early reduction is consistent with active redistribution of activated T cells from peripheral circulation into the tumor site and draining lymph nodes, rather than immune suppression, and is further supported by the concurrent systemic IFN-γ suppression observed in serum cytokine profiling at the same timepoint. The parallel decline in IL-2-secreting T cells suggests that peripheral T cells had undergone activation-driven consumption of IL-2 and subsequent trafficking to the tumor microenvironment, where local proliferation would not be captured by PBMC sampling. By the fifth injection triple combination therapy group demonstrating higher counts of both IFN-γ- and IL-2-secreting T cells compared to all other treatment groups. This late-phase superiority indicates presumably that the combination regimen generated a robust systemic pool of tumor-educated effector T cells, consistent with the synergistic delivery of GCV-driven immunogenic cell death —hopefully providing broad tumor antigen release for T cell priming — and VV-mIL15Rα-mediated IL-15Rα transpresentation, which could further selectively amplify CD8+ memory T cell and NK cell survival. The magnitude of peripheral T cell reconstitution in the combination group correlated directly with the most pronounced tumor volume reduction observed across all experimental arms, providing cellular-level evidence supporting the superior therapeutic efficacy of this regimen.

2.5. Systemic Cytokine Response Following Repeated Administration of Recombinant LIVP Strains

To characterize the systemic immune landscape triggered by combined virotherapy, serum cytokine profiles were analyzed 24 h post-prime (1st injection) and post-boost (5th injection) in 4T1 tumor-bearing mice. The cohorts were treated with VV-HSVtk, VV-mIL15Ra or its' combinations, with or without ganciclovir (GCV). The evaluated multiplex panel encompassed pro-inflammatory mediators, Th1-associated cytokines, Th17/epithelial alarmins, and immunoregulatory factors (Figure 4A-C).

Overall, therapeutic intervention elicited a robust systemic cytokine flux; however, the profile diverged from a canonical cytotoxic anti-tumor signature. Instead, the response manifested as a complex hybrid state characterized by acute inflammatory activation, partial Th1/NK-cell stimulation, and the concomitant induction of immunoregulatory and tumor-supportive mediators.

 doi:10.20944/preprints202605.0960.v1

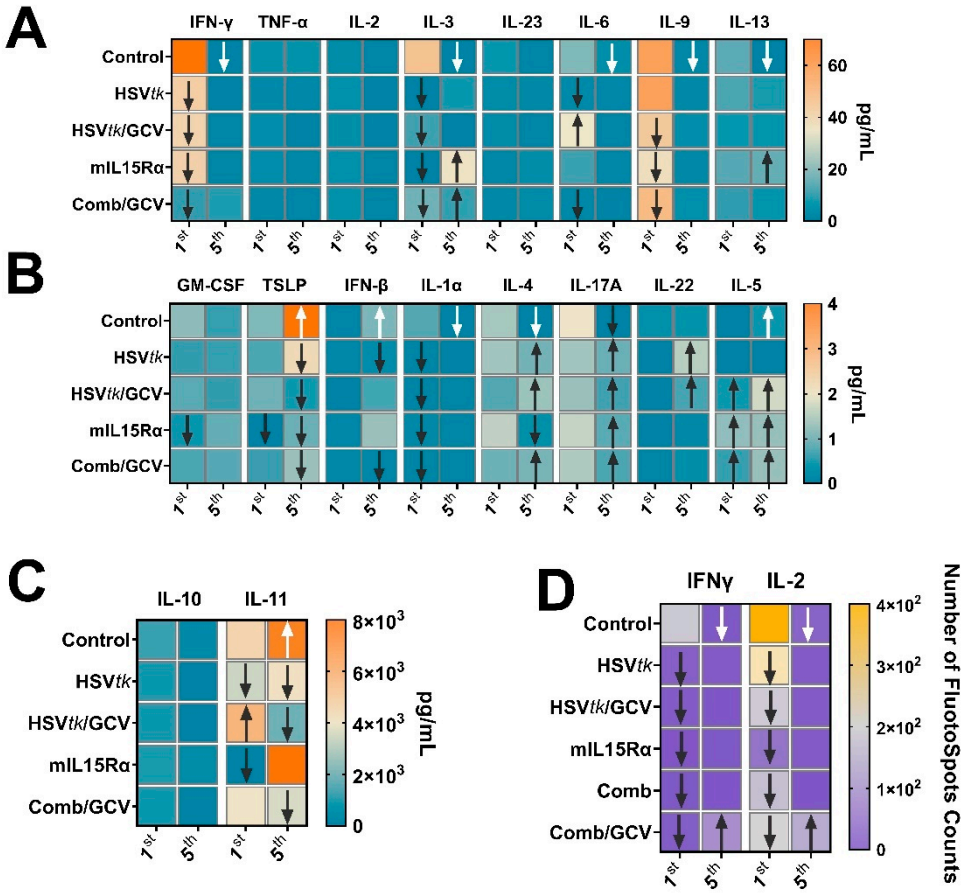

Figure 4. (a-c) - Assessment of cytokine dynamic in serum of treated animals, grouped by average concentration; (d) - analysis of activated circulating lymphocytes.

Serum cytokine profiling revealed that treatment groups induced distinct and heterogeneous immune signatures rather than a uniform cytokine response. Following the first therapeutic injection, the VV-mIL15Rα group exhibited elevated IL-5 alongside reduced IFN-γ, IL-1α, IL-3, IL-4, IL-9, TSLP, GM-CSF, and IL-11. The VV-HSVtk group was characterized by decreased IFN-γ, IL-1α, IL-3, IL-6, and IL-11. The VV-HSVtk+GCV group demonstrated decreased IFN-γ, IL-1α, IL-3, and IL-9, concurrent with elevated IL-5, IL-6, and IL-11. The combination of both viruses with GCV increased IL-5 while decreasing IFN-γ, IL-1α, IL-3, IL-6, and IL-9.

At the end of therapy, when pronounced antitumor effects were observed, differences in serum cytokine concentrations relative to the control group were less obvious overall, yet qualitatively more informative. Following the fifth injection, the VV-mIL15Rα group exhibited elevated IL-3, IL-5, IL-13, and IL-17A, with reduced IL-4 and TSLP. The VV-HSVtk group was characterized by increased IL-4, IL-17A, and IL-22, alongside decreased IL-11, TSLP, and IFN-β. The VV-HSVtk/GCV group showed decreased TSLP and IL-11, together with elevated IL-4, IL-5, IL-17A, and IL-22. The combination of both viruses with GCV increased IL-3, IL-4, IL-5, and IL-17A while decreasing TSLP, IFN-β, and IL-11. Taken together, these data demonstrate that the dual-virus combination with GCV uniquely integrates cytokine changes that are only partially recapitulated by each monotherapy arm, suggesting synergistic and mechanistically distinct immune remodeling that correlates with the observed dramatic reduction in tumor volume and complete responses in a subset of treated animals.

2.6. Combined Therapy Leads to Enhanced Tumor Necrosis and Immune Infiltration,

The histological analysis (Figure 5) of tumor necrosis in the combination and combination/GCV groups is consistent with enhanced local tumor destruction in these arms, with absence of spleen and

 doi:10.20944/preprints202605.0960.v1

hepatic pathology, this result is alights which previous described safety profile of the LIVP strain, which shows natural selectivity for tumor cells [22]. In prior studies, HSVtk-based suicide gene therapy combined with cytokine gene strategies increased antitumor efficacy and could enhance both local and distant tumor control, supporting the biological plausibility of the current findings. Overall, the data suggest that the combined treatment strategies induced local tumor injury together with systemic immune activation, but also engaged compensatory cytokine networks that likely modulated the magnitude and quality of the response [23].

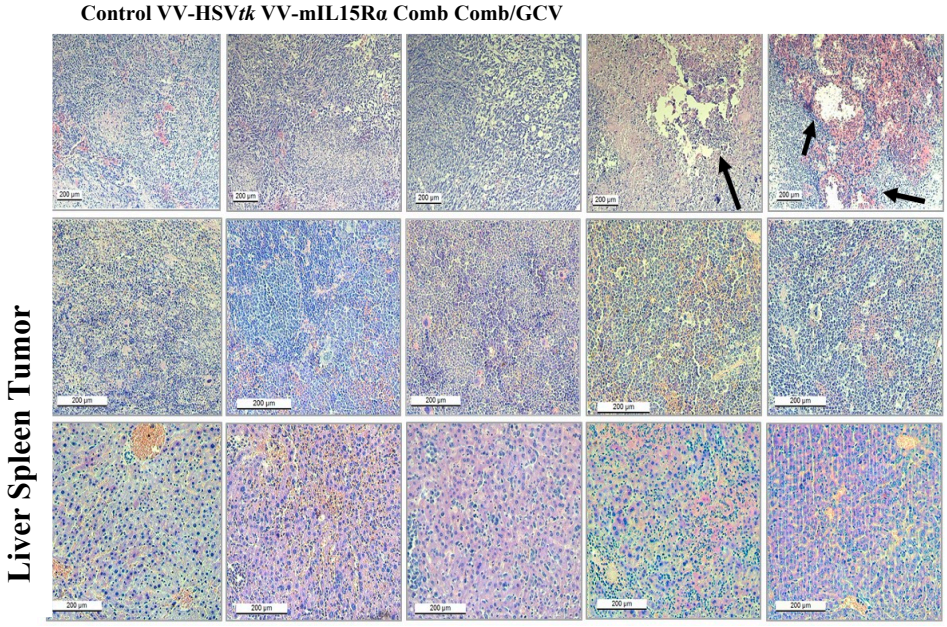

Figure 5. Histological analysis of tumor, spleen and liver in treated animals, necrosis foci are marked with arrows.

Immunohistochemical staining for CD4 and CD8 (Figure S4) further supported cytokine profiling data by showing treatment-dependent changes in the tumor immune infiltrate. In tumors of control animals, specific CD4 or CD8 signal was essentially absent, indicating a lack of appreciable T-cell infiltration. In contrast, the combination/GCV group showed a more pronounced presence of both CD4+ and CD8+ cells, suggesting stronger recruitment of adaptive immune cells into the tumor site. The HSVtk/GCV group also showed CD4+ and CD8+ cells, but the number of cells and signal was weaker than in the combination/GCV group, indicating more limited level of T-cell infiltration. This pattern was consistent with the increased IFN-γ response observed in the combination/GCV group and with the elevated IL-2 production detected in spleen cells at the end of treatment, supporting systemic T-cell activation. ICC showed heterogeneous staining pattern, with different tumor regions containing either CD4+ or CD8+ cells. This uneven distribution suggests that the immune response was spatially variable within the tumor microenvironment and most likelywas not limited to a single T-cell subset. Such a pattern matches the mixed cytokine profile observed in serum, including increased IL-4, IL-5 and IL-17A together with decrease of IFNβ and TSLP. Overall, these findings indicate that treatment altered both the systemic cytokine milieu and the local cellular composition of the tumor microenvironment.

3. Discussion

The present study demonstrates that integration of metabolic suicide gene therapy with cytokine-receptor modulation within the LIVP vaccinia virus backbone establishes a synergistic therapeutic window that neither strategy achieves independently. Although oncolytic viruses are inherently immunogenic [24,25], single-agent oncolytic virotherapy is frequently constrained by

 doi:10.20944/preprints202605.0960.v1

antiviral host defense mechanisms, acquired resistance, and intrinsic tumor heterogeneity and the physical barriers imposed by extracellular matrix remodeling, stromal fibrosis, and tumor necrosis [26–29]. Our findings indicate that the triple combination of VV-HSVtk, VV-mIL15Rα, and ganciclovir (GCV) simultaneously addresses these limitations by coupling direct tumor reduction with reversal of systemic immune evasion.

The primary obstacle in treating aggressive models such as 4T1 triple-negative breast cancer is the profoundly immunosuppressive tumor microenvironment (TME), which actively excludes and exhausts infiltrating effector lymphocytes [30,31]. Our in vitro data establish the potency of the HSVtk/GCV bystander effect as the mechanistic foundation of this approach. In contrast to conventional oncolysis, which requires productive viral infection of individual tumor cells, HSVtk-mediated phosphorylation of GCV generates diffusible cytotoxic nucleoside analogues capable of destroying neighboring non-infected malignant cells [15,32]. This metabolic direct cell death not only reduces tumor burden but releases a coordinated wave of tumor-associated antigens (TAAs) and damage-associated molecular patterns (DAMPs) — including HMGB1, and extracellular ATP — effectively converting an immunologically silent "cold" tumor into an antigen-rich, DC-activating "hot" environment permissive to adaptive immune priming [25,33–36].

However, antigen release alone is insufficient to sustain long-term remission when the host immune system remains functionally suppressed. This is the critical niche occupied by VV-mIL15Rα as a part od combined therapy. Unlike soluble IL-15, which is subject to rapid proteolytic degradation and limited bioavailability in the circulation, expression of the membrane-anchored IL-15 receptor α subunit facilitates the assembly of high-affinity IL-15/IL15Rα trans-presentation complexes on the surface of antigen-presenting cells, delivering a qualitatively superior and spatially focused activation signal to NK cells and $CD8^+$ T cells [37–39].

A notable finding from our in vitro co-culture experiments was that, while combination virus treatment did not substantially amplify direct viral oncolysis beyond monotherapy, the addition of donor-derived NK cells produced a marked and synergistic increase in tumor cell death. This dissociation between viral cytolytic activity and immune-mediated killing reveals an important mechanistic principle: VV-mIL15Rα functions as an immunological bridge, sensitizing the tumor to innate effector mechanisms that would otherwise be functionally excluded from the immunosuppressive TME. The IL-15 trans-presentation signal lowers the activation threshold of NK cells, enabling recognition and elimination of virally infected and antigen-exposed tumor cells that resist direct oncolysis [39,40].

Consistent with this mechanisms, our in vivo data, systemic cytokine profiling, and FluoroSpot analysis suggest enhanced systemic immune activation, while tumor CD4/CD8 staining is consistent with increased T-cell presence within the tumor microenvironment, accompanied by compartmentalized immune activation characterized by enhanced peripheral blood IL-2 and IFN-γ activated cells— a potential pattern indicative of active effector lymphocyte extravasation and tumor-directed trafficking [31,41]. All groups share early suppression of IFN-γ, IL-1α, and IL-3, reflecting vaccinia-encoded immunoevasins including the B8R IFN-γ decoy receptor and vCKBP chemokine-binding proteins [42]. The combination uniquely adds early co-elevation of IL-5, IL-6, and IL-11 — absent from VV-mIL15Rα alone (which suppresses IL-11) and inverted in VV-HSVtk alone (which suppresses IL-6). This divergence is logically explained by GCV-driven immunological cell death adding an inflammatory layer that the virus alone cannot generate without the cytotoxic prodrug. The unique suppression of IL-9 only in combination groups further suggests deeper remodeling of the mast cell and regulatory T cell compartments requiring simultaneous activity of both viral transgenes [43]. By the fifth injection, the shared rise in IL-17A and fall in TSLP across all effective groups reflects the progressive collapse of stromal immune tolerance. TSLP, produced by tumor-associated stroma, drives tolerogenic dendritic cell programming that suppresses effector T cell differentiation; its cumulative suppression by repeated virotherapy derepresses Th17 expansion and antitumor neutrophil and γδ T cell activity. The concurrent downregulation of IL-11 — a CAF-derived STAT3 activator that promotes tumor survival and pre-metastatic niche formation [44,45] —

 doi:10.20944/preprints202605.0960.v1

indicates active dismantling of the CAF-driven stromal support network that enables 4T1 metastasis. Paradoxically, late IFN-β suppression in HSVtk-containing groups could potentially reflect a successful shift from antiviral to antitumor immune mode, facilitated by vaccinia E3L and K3L gene products that antagonize PKR-mediated IFN-β signaling [46] and allow sustained intratumoral viral replication[44,47,48]. The late-phase IL-5 elevation, co-occurring with IL-17A rise and TSLP suppression, is not a tolerogenic Th2 signal but rather marks eosinophil mobilization as a non-classical cytotoxic arm. Tumor-infiltrating eosinophils kill tumor cells via perforin, granzyme, and reactive oxygen species, and remodel the TME through CXCL9/CXCL10 secretion that amplifies CD8+ T cell recruitment [49,50]. IL-22 elevation in HSVtk-containing groups further sensitizes residual tumor cells to immune killing by upregulating MHC class I and NK cell stress ligands. Together, these signals establish a converging Th2/Th17 effector state that simultaneously deploys eosinophils, neutrophils, cytotoxic T cells, and NK cells — a multi-arm response that neither monotherapy can achieve and that mechanistically accounts for the dramatic tumor volume reduction and complete responses observed in the 4T1 model [51,52].

These systemic changes closely align with the local histological and immunohistochemical findings. The triple combination with GCV produced the most extensive tumor necrosis and the highest density of intratumoral $CD4^+$ and $CD8^+$ T cells, whereas tumors from control animals were essentially devoid of T-cell infiltrates. The HSVtk/GCV group also displayed $CD4^+$ and $CD8^+$ cells within the tumor, but at lower abundance than in the triple combination group, indicating that metabolic debulking alone can partially remodel the tumor microenvironment, yet optimal conversion of "cold" 4T1 tumors into a T-cell-inflamed state requires concomitant IL-15 pathway activation. This pattern is consistent with earlier studies of IL-15/IL-15Rα-armed OVs, where increased $CD8^+$ T-cell infiltration correlated with improved tumor regression and survival [11]. The more heterogeneous distribution of $CD4^+$ and $CD8^+$ cells observed in the single-agent HSVtk and mIL-15Rα groups suggests spatially variable immune engagement, mirroring the mixed cytokine profiles and underscoring the importance of combining metabolic and immunologic mechanisms within a single therapeutic scheme.

Histological examination of liver and spleen from treated animals revealed no overt pathological abnormalities following repeated intertumoral administration, confirming that the recombinant LIVP variants did not produce detectable off-target organ toxicity under the conditions tested [11]. This safety profile is consistent with the established tropism of attenuated vaccinia virus strains for metabolically active tumor tissue and further supports the translational potential of this platform.

When viewed in the context of related approaches, our data support a model in which integrating HSVtk/GCV suicide gene therapy with IL-15Rα-targeted immunomodulation within a vaccinia backbone yields additive or synergistic benefits over either strategy alone. IL-15- and IL-15/IL-15Rα-armed OVs based on vaccinia, vesicular stomatitis virus, myxoma virus, and adenoviral vectors have demonstrated the ability to expand cytotoxic lymphocytes and generate systemic tumor immunity, particularly in combination with PD-1/PD-L1 or CTLA-4 blockade [6,53–56]. In parallel, HSVtk/GCV systems delivered by adenoviral or retroviral vectors have shown potent local tumor killing and bystander effects in multiple preclinical models and early clinical studies [20]. Our work brings these principles together in a single LIVP-based platform and demonstrates efficacy in a stringent 4T1 triple-negative breast cancer model that is resistant to many immunotherapeutic interventions. Notably, we used two coordinated but genetically distinct viral strains, separating metabolic and cytokine-receptor functions. This division-of-labor strategy, also explored in previous LIVP IL-15/IL-15Rα work, offers modularity and may reduce fitness costs associated with large multigenic inserts, but it also raises questions about optimal dosing ratios, scheduling, and potential competition between variants that warrant further investigation.

4. Materials and Methods

4.1. Generation of Recombinant Viruses

 doi:10.20944/preprints202605.0960.v1

LIVP strain with disruption of TK and expression of tagRFP reporter gene under the control of 7.5k promoter (VV-RFP) and mIL-15Rα were constructed and described previously [11,57]. To construct HSVtk expressing variant DNA was extracted from HEK293T cells infected with HSV type 1 at MOI=1 24 hours after infection using phenol-chloroform method as previously described [58]. Next using Q5 High Fidelity polymerase (NEB, USA) HSVtk gene was amplified and cloned by sticky ends ligation into the recombination plasmid previously developed at the Cell Proliferation laboratory EIMB RAS [59]. Transfection for recombination was performed using PEI in HEK293T cells as described before [60], the cells were infected with LIVP strain at MOI=1. TK-disrupted recombinant variants were selected on Rat-2 TK-minus− cells (deficient in the TK expression) treated with 2-bromodeoxyuridine after infection at MOI 1 of the virus variants gained after transfection, separated by plaque assay and cloned. Insertion was confirmed by sequencing of amplified TK locus from viral genomic DNA. Recombinant viruses were propagated in BHK21 cells and purified by the sucrose gradient method for in vitro and in vivo experiments [61].

4.2. Cell Lines and Culture Conditions

Baby hamster kidney BHK-21 (CCL-10 ATCC) cells, 4T1 murine breast adenocarcinoma cells (CRL-3406 ATCC) and a panel of human cancer cell lines—including HeLa, HEK293T, HCT116, NCI-H460, TOV21G, DU145, MCF7, and C33A—were obtained from the collection of laboratory of cell proliferation (EIMB RAS, Moscow, Russia). CT2A murine glioma CT-2A murine glioma cell lines were kindly provided by Dr. Aleksei A. Stepanenko (Department of Fundamental and Applied Neurobiology, Serbsky National Medical Research Center for Psychiatry and Narcology, Moscow, Russia). Cells were maintained in Dulbecco's Modified Eagle's Medium (DMEM/Glutamax; Servicebio, Wuhan, China), supplemented with 10% fetal bovine serum (FBS, HyClone, Cytiva, Logan, UT, USA) and penicillin-streptomycin at standard concentrations (PanEco, Moscow, Russia). Human NK cells for co-culture assays were isolated from healthy donor PBMCs and kindly gifted by professor Vladimir Baklaushev.

4.3. In Vitro Cytotoxicity and NK Cell Co-Culture

Cell viability was evaluated using the Resazurin (Alamar Blue) assay. Cells were seeded in 96-well plates and infected with VV-HSVtk-RFP or VV-RFP at wide range of MOI (0,001, 0,01, 0,1, 1, 10, 100). At 24 h post-infection, Ganciclovir (GCV) was added at concentrations of 12,5, 25, 50, and 100 μM. Resazurin (0.15 mg/mL; Sigma-Aldrich) was added to each well, and absorbance was measured at 24, 48, 72, and 96h. For NK cells co-cultivation MOI=1 was used, preinfected cells were added with Effector:Target (E:T) cells at ratio of 5:1 at 24 h post-infection alongside with GCV treatment.

4.4. RT-qPCR

Total RNA was isolated from 4*105 cells infected with VV-HSVtk using ExtractRNA reagent and CleanRNA Standard kit (Evrogen, Moscow, Russia), followed by DNase I treatment (Thermo Fisher Scientific). cDNA was synthesized using SuperScript III Reverse Transcriptase (Invitrogen) and random octamer primers per the manufacturer's protocol. qPCR was conducted on a CFX96 Touch System (Bio-Rad) with qPCRmix-HS SYBR (Evrogen) and gene-specific primers (Table S1), validated for specificity via melting curve analysis (single peaks, no non-specific products) and efficiency through serial cDNA dilutions (R2>0.98 for all pairs). Relative expression was calculated by the comparative ΔCt method [62], using β-actin as internal controls. Fold changes in gene expression were calculated using the 2-ΔCt method.

4.5. Assessment of Therapeutic Efficacy In Vivo

The anti-tumor efficacy was evaluated in the syngeneic BALB/c murine 4T1 mammary carcinoma model. Animals were divided into eight essential treatment groups (Table 1):

 doi:10.20944/preprints202605.0960.v1

Table 1. Treatment groups.

Group	Treatment Components	Primary Function
1	Control (Saline)	Baseline
2	Ganciclovir (GCV)	Prodrug toxicity control
3	VV-HSVtk	TAA release
4	VV-mIL15Rα	Immune stimulation
5	VV-HSVtk/GCV	GDEPT + Oncolysis
6	VV-mIL15Rα /GCV	Immune stimulation + (GCV control)
7	VV-HSVtk + VV-mIL15Rα	Combined Oncolysis/TAA/Immune
8	VV-HSVtk + VV-mIL15Rα/GCV	GDEPT + Synergistic Immune Boost

All animal procedures were approved by the EIMB Institutional Animal Care and Use Committee (Protocol No. 1 issued on March 05th, 2025). Female and male 6-week-old Balb/c mice were used for 4T1 models. Once tumors reached approx 50 mm^3, mice were randomized into eight groups: Saline, GCV only, VV-HSVtk, VV-mIL15r, VV-HSVtk/GCV, VV-mIL15Rα/GCV, VV-HSVtk + VV-mIL15r, and the Triple Combination (VV-HSVtk + VV-mIL15ra + GCV). Viruses were administered intratumorally five times every 4 days ($2*10^7$ PFU of total dose). In GCV-treated groups, GCV (50 mg/kg) was injected intraperitoneally 48 h after each virus administration. Tumor volume was measured by calipers every other day and calculated as $V = (Length*Width^2) / 2$.

4.6. PBMC Isolation and Preparation

Mouse peripheral blood were harvested into sterile microcentrifuge tubes pre-treated with EDTA as an anticoagulant, PBMCs were isolated via Ficoll-PaQue density gradient centrifugation (1,800 350× g, 20 min, no brake), followed by washing in PBS + 2% FBS. Cells were resuspended at 5-10 × 10^6/5/mL in freezing medium (9030% FBS + 10% DMSO), aliquoted into cryovials, and cryopreserved using a controlled-rate freezer (-1°C/min to -80°C) prior to transfer to liquid nitrogen for retrospective ELISPOT analysis. At the day of experiment gently defrizzed. The resulting splenocytesPBMCs were washed and resuspended in complete DMEM medium supplemented with 10% fetal bovine serum (FBS) and 1% penicillin-streptomycin at standart concentrations. Cell viability and density were determined via trypan blue exclusion using an automated cell counter Luna II (RWD Life Science, China).

4.7. Fluorospot Analysis

To quantify the frequency of polyfunctional T-cell populations, a triple-color mouse FluoroSpot assay (Mabtech AB, Sweden) was performed to simultaneously detect IFN-γ, IL-2, and TNF-α at the single-cell level. The plates were washed and blocked with complete DMEM medium containing 10% FBS for at least 30 minutes at room temperature. Splenocytes were seeded at a density of 2.5x105 cells/well in triplicate. To support the detection of cytokines from pre-activated T cells, monoclonal anti-CD28 (0.1 μg/mL) was added to all cell-containing wells as a costimulatory signal. Wells containing recombinant mouse IFN-γ, IL-2, and TNFα were processed in parallel as positive controls to validate the performance of the detection reagents and the accuracy of the fluorescent signal co-localization. After 24 h of incubation at 37°C in 5% CO_2, the cells were removed, and the plates were developed using a cocktail of specific detection antibodies: biotinylated anti-IFN-γ (R4-6A2), BAM-conjugated anti-IL-2 (MT156B6), and WAV-conjugated anti-TNF-α (MT25C5). After 2 h, the membranes were washed and incubated for 1 h with a fluorophore-conjugated secondary cocktail consisting of Streptavidin-490, anti-BAM-550, and anti-WAV-640. Finally, the plates were treated with a fluorescence enhancer for 15 minutes, dried in the dark, and analyzed using an automated reader. Spot-forming cells (SFCs) and polyfunctional "multi-spot" populations were enumerated by identifying spatially co-localized signals across the 490 nm, 550 nm, and 640 nm channels, with values expressed as SFCs per $3*10^5$ PBMCs after background subtraction.

 doi:10.20944/preprints202605.0960.v1

4.8. Serum Collection and Processing

To monitor the systemic cytokine response throughout the treatment course, blood samples were collected from the tail vein of 4T1-tumor-bearing mice 24 hours after each of the five viral administrations. To ensure adequate blood flow and minimize animal distress, mice were briefly warmed under a heat lamp or in a warming chamber prior to the procedure. Approximately 50–100 µl of whole blood was collected into sterile microcentrifuge tubes pre-treated with EDTA as an anticoagulant. The samples were then subjected to centrifugation at 2,000 x g for 10 minutes at 4°C to separate the cellular components. The resulting supernatant was carefully aspirated, and the serum fractions were aliquoted and stored at -80°C to preserve cytokine stability until further multiplex analysis. All procedures were performed in accordance with institutional animal welfare guidelines to ensure minimal distress to the mice during repeated sampling.

4.9. Multiplex Cytokine Quantification (LEGENDplex™)

Systemic cytokine concentrations were quantified using bead-based multiplex immunoassays. Serum samples were analyzed using the LEGENDplex™ Mouse Cytokine Panel 2 (Standard V02) and the LEGENDplex™ Mouse Th Cytokine Panel (12-plex) with V-bottom plate (VbP) (Cat. No. 741038, Version V03, 100 tests) (BioLegend, San Diego, CA, USA) according to the manufacturer's instructions.

The combined panels allowed for the simultaneous detection of a broad range of analytes, including pro-inflammatory cytokines, Th-associated mediators, and immunoregulatory factors. Briefly, serum samples were incubated with cytokine-specific capture beads, which are distinguished by their size and internal fluorescence intensities. Following the primary incubation, biotinylated detection antibodies were added to form sandwich complexes, followed by the addition of Streptavidin-Phycoerythrin (SA-PE) to provide a fluorescent signal proportional to the amount of bound analyte.

Data acquisition was performed using a BD LSRFortessa™ flow cytometer. A minimum of 2000 beads per analyte were collected to ensure statistical robustness. The raw fluorescence intensities were processed using the LEGENDplex™ Data Analysis Software, where cytokine concentrations were calculated by interpolation from a five-parameter logistic (5PL) standard curve. All samples were run in duplicate, and values were expressed in pg/mL.

4.10. ICC and IHC Analyses

For histological analysis, subcutaneous tumors, livers and spleens were collected and fixed in 4% paraformaldehyde at 4°C overnight. In 16 hours, tissue samples were embedded in paraffin, serial 5 µm sections were prepared using a rotary microtome (Leica Microsystems, USA) and stained with hematoxylin and eosin (H&E) according to standard protocols [63].

Tumor immune cells infiltration was assessed on coronal 50 µm cryosections (Leica VT1200 S vibratome), permeabilized in 0.1% Triton X-100 and blocked with 1% goat serum. Sections were incubated overnight at 4°C with: Alexa Fluor 488 anti-mouse CD4 (100423, Biolegend) and eFluor 660 CD8a (AMC908, eBioscience) Images were acquired using a Nikon A1R confocal laser scanning microscope (Nikon, Japan).

4.11. Statistical Analysis

Statistical processing was performed using GraphPad Prism version 10.1.2 (GraphPad Software, San Diego, CA, USA). Data normality was assessed prior to analysis, and results are expressed as mean ± standard deviation (SD). For comparisons between multiple experimental groups, a one-way or two-way analysis of variance (ANOVA) was employed, followed by appropriate post-hoc tests for multiple comparisons. Log-rank test was used for survival analysis. Differences were considered statistically significant at: *, $p < 0.05$; **, $p < 0.01$; ***, $p < 0.001$, ***, $p < 0.0001$.

 doi:10.20944/preprints202605.0960.v1

5. Conclusions

Collectively, these findings establish that the coordinated deployment of HSVtk/GCV-mediated cytotoxic bystander killing and mIL-15Rα-driven immune co-stimulation within a recombinant LIVP vaccinia virus platform produces complementary and mutually reinforcing anti-tumor mechanisms. Metabolic debulking generates the immunogenic cell death and antigen landscape required for adaptive immune priming, while IL-15 trans-presentation sustains the NK cell and $CD8^+$ T cell effector populations needed to execute and perpetuate that response. The result is delayed tumor progression, prolonged survival, and increased tumor regression in the aggressive syngeneic 4T1 model — an outcome that neither component achieved as monotherapy. Beyond their immediate therapeutic significance, these results provide a mechanistic rationale for the broader development of multimodal armed vaccinia virus platforms in which direct cytotoxicity and immunostimulatory transgene expression are engineered to act in concert. Future studies should evaluate this combination in orthotopic and metastatic settings, explore the durability of immunological memory generated, and assess synergy with systemic checkpoint inhibition — an approach whose efficacy is likely to be substantially enhanced by the TME remodeling demonstrated here.

Supplementary Materials: The following supporting information can be downloaded at the website of this paper posted on Preprints.org, Figure S1: Sensitivity of cells to VV-HSVtk and VV-RFP in presence or absence of GCV; Figure S2: Relative expression of HSVtk in infected cells 24 and 48 hours post infection; Figure S3: Pictures of tumor regression after treatment; Figure S4: Immunofluorescent detection of CD4+ and CD8+ cells in 4T1 tumors after treatment. Representative fluorescence images show infiltration of CD8+ (red) and CD4+ cells (green) in group with triple combination treatment. Scale bar, 50 μm; Table S1: Primers for RT-PCR.

Author Contributions: Conceptualization, O.A., P.V. and A.P.; methodology, O.A., P.V., M.V., D.K. and A.P.; formal analysis, O.A. and A.P.; investigation, O.A., P.V., M.V., S.I., Ya.S., V.V., D.K., V.K., and A.P.; resources, V.B. and A.P.; writing – original draft preparation, O.A, A.P.; writing – review and editing, O.A., P.V., M.V., D.K., A.S, S.A, P.C. and A.P.; supervision, A.P.; project administration, A.P.; funding acquisition, P.C. and A.P. All authors have read and agreed to the published version of the manuscript.

Funding: The viral strain generation and cytotoxicity studies and histology were funded by the Russian Science Foundation (grant #23-74-10102); in vivo studies were funded by Ministry of Science and Higher Education of the Russian Federation (Federal scientific and technical program for the development of genetic technologies for 2019–2030, agreement #075-15-2025-519).

Institutional Review Board Statement: All animal studies were approved by the Ethical Committee of the Engelhardt Institute of Molecular Biology, Moscow, Russia (Protocol No. 1 issued on March 05th, 2025).

Informed Consent Statement: Not applicable.

Data Availability Statement: The original contributions presented in this study are included in the article/supplementary material. Further inquiries can be directed to the corresponding authors.

Acknowledgments: We express our sincere gratitude to professor Vladimir Baklaushev for kindly providing NK cells, as well as to professor Alexander Ivanov for his invaluable assistance and support in conducting this study.

Conflicts of Interest: The authors declare no conflict of interest.

Abbreviations

The following abbreviations are used in this manuscript:

GCV	Ganciclovir
DAMPs	Damage associated molecular patterns
HSVtk	Herpes simplex virus thymidine kinase
i.t.	Intratumoral

 doi:10.20944/preprints202605.0960.v1

i.p.	Intraperinatal
ICC	Immunocytochemistry
IHC	Immunohistochemistry
LIVP	Lister (strain) Institute of Viral Preparation
MHC	Major histocompatibility complex
MOI	Multiplicity of infection
NK	Natural killer
OVs	Oncolytic viruses
TAAs	Tumor-associated antigens
TCID50	50% tissue culture infectious dose
TK	Thymidine kinase
TME	Tumor microenvironment
TNBC	Triple-negative breast cancer
VV	Vaccinia virus

References

1. Lin, D.; Shen, Y.; Liang, T. Oncolytic virotherapy: basic principles, recent advances and future directions. *Signal Transduct Target Ther* **2023**, *8*, 156, doi:10.1038/s41392-023-01407-6.
2. Alekseeva, O.N.; Hoa, L.T.; Vorobyev, P.O.; Kochetkov, D.V.; Gumennaya, Y.D.; Naberezhnaya, E.R.; Chuvashov, D.O.; Ivanov, A.V.; Chumakov, P.M.; Lipatova, A.V. Receptors and Host Factors for Enterovirus Infection: Implications for Cancer Therapy. *Cancers (Basel)* **2024**, *16*, doi:10.3390/cancers16183139.
3. Li, R.; Zhang, J.; Gilbert, S.M.; Conejo-Garcia, J.; Mule, J.J. Using oncolytic viruses to ignite the tumour immune microenvironment in bladder cancer. *Nat Rev Urol* **2021**, *18*, 543-555, doi:10.1038/s41585-021-00483-z.
4. Johnson, D.B.; Puzanov, I.; Kelley, M.C. Talimogene laherparepvec (T-VEC) for the treatment of advanced melanoma. *Immunotherapy* **2015**, *7*, 611-619, doi:10.2217/imt.15.35.
5. Shakiba, Y.; Vorobyev, P.O.; Mahmoud, M.; Hamad, A.; Kochetkov, D.V.; Yusubalieva, G.M.; Baklaushev, V.P.; Chumakov, P.M.; Lipatova, A.V. Recombinant Strains of Oncolytic Vaccinia Virus for Cancer Immunotherapy. *Biochemistry (Mosc)* **2023**, *88*, 823-841, doi:10.1134/S000629792306010X.
6. Liu, Z.; Ge, Y.; Wang, H.; Ma, C.; Feist, M.; Ju, S.; Guo, Z.S.; Bartlett, D.L. Modifying the cancer-immune set point using vaccinia virus expressing re-designed interleukin-2. *Nat Commun* **2018**, *9*, 4682, doi:10.1038/s41467-018-06954-z.
7. Jackaman, C.; Nelson, D.J. Cytokine-armed vaccinia virus infects the mesothelioma tumor microenvironment to overcome immune tolerance and mediate tumor resolution. *Cancer Gene Ther* **2010**, *17*, 429-440, doi:10.1038/cgt.2009.85.
8. Yang, M.; Chen, S.; Du, J.; He, J.; Wang, Y.; Li, Z.; Liu, G.; Peng, W.; Zeng, X.; Li, D.; et al. NK cell development requires Tsc1-dependent negative regulation of IL-15-triggered mTORC1 activation. *Nat Commun* **2016**, *7*, 12730, doi:10.1038/ncomms12730.
9. Perera, P.Y.; Lichy, J.H.; Waldmann, T.A.; Perera, L.P. The role of interleukin-15 in inflammation and immune responses to infection: implications for its therapeutic use. *Microbes Infect* **2012**, *14*, 247-261, doi:10.1016/j.micinf.2011.10.006.
10. Kowalsky, S.J.; Liu, Z.; Feist, M.; Berkey, S.E.; Ma, C.; Ravindranathan, R.; Dai, E.; Roy, E.J.; Guo, Z.S.; Bartlett, D.L. Superagonist IL-15-Armed Oncolytic Virus Elicits Potent Antitumor Immunity and Therapy That Are Enhanced with PD-1 Blockade. *Mol Ther* **2018**, *26*, 2476-2486, doi:10.1016/j.ymthe.2018.07.013.
11. Shakiba, Y.; Vorobyev, P.O.; Yusubalieva, G.M.; Kochetkov, D.V.; Zajtseva, K.V.; Valikhov, M.P.; Kalsin, V.A.; Zabozlaev, F.G.; Semkina, A.S.; Troitskiy, A.V.; et al. Oncolytic therapy with recombinant vaccinia viruses targeting the interleukin-15 pathway elicits a synergistic response. *Mol Ther Oncolytics* **2023**, *29*, 158-168, doi:10.1016/j.omto.2023.05.002.
12. Zarogoulidis, P.; Darwiche, K.; Sakkas, A.; Yarmus, L.; Huang, H.; Li, Q.; Freitag, L.; Zarogoulidis, K.; Malecki, M. Suicide Gene Therapy for Cancer - Current Strategies. *J Genet Syndr Gene Ther* **2013**, *4*, doi:10.4172/2157-7412.1000139.

 doi:10.20944/preprints202605.0960.v1

13. Islam, S.; Lee, B.; Jiang, F.; Kim, E.K.; Ahn, S.C.; Hwang, T.H. Engineering and Characterization of Oncolytic Vaccinia Virus Expressing Truncated Herpes Simplex Virus Thymidine Kinase. *Cancers (Basel)* **2020**, *12*, doi:10.3390/cancers12010228.
14. Wildner, O.; Blaese, R.M.; Morris, J.C. Therapy of colon cancer with oncolytic adenovirus is enhanced by the addition of herpes simplex virus-thymidine kinase. *Cancer Res* **1999**, *59*, 410-413.
15. Touraine, R.L.; Ishii-Morita, H.; Ramsey, W.J.; Blaese, R.M. The bystander effect in the HSVtk/ganciclovir system and its relationship to gap junctional communication. *Gene Ther* **1998**, *5*, 1705-1711, doi:10.1038/sj.gt.3300784.
16. Kochneva, G.; Zonov, E.; Grazhdantseva, A.; Yunusova, A.; Sibolobova, G.; Popov, E.; Taranov, O.; Netesov, S.; Chumakov, P.; Ryabchikova, E. Apoptin enhances the oncolytic properties of vaccinia virus and modifies mechanisms of tumor regression. *Oncotarget* **2014**, *5*, 11269-11282, doi:10.18632/oncotarget.2579.
17. Maruri-Avidal, L.; Limsirichai, P.; Gulizia, N.; Kirn, D.H. Intravenous oncolytic vaccinia expressing transgenes for enhanced safety, inhibition of shedding, imaging, and systemic cancer immunotherapy. *Mol Ther Oncol* **2026**, *34*, 201153, doi:10.1016/j.omton.2026.201153.
18. Fretwell, E.C.; Houldsworth, A. Oncolytic Virus Therapy in a New Era of Immunotherapy, Enhanced by Combination with Existing Anticancer Therapies: Turn up the Heat! *J Cancer* **2025**, *16*, 1782-1793, doi:10.7150/jca.102285.
19. Su, J.; Song, Y.; Zhu, Z.; Huang, X.; Fan, J.; Qiao, J.; Mao, F. Cell-cell communication: new insights and clinical implications. *Signal Transduct Target Ther* **2024**, *9*, 196, doi:10.1038/s41392-024-01888-z.
20. Greco, R.; Oliveira, G.; Stanghellini, M.T.; Vago, L.; Bondanza, A.; Peccatori, J.; Cieri, N.; Marktel, S.; Mastaglio, S.; Bordignon, C.; et al. Improving the safety of cell therapy with the TK-suicide gene. *Front Pharmacol* **2015**, *6*, 95, doi:10.3389/fphar.2015.00095.
21. Xie, H.; Xi, X.; Lei, T.; Liu, H.; Xia, Z. CD8(+) T cell exhaustion in the tumor microenvironment of breast cancer. *Front Immunol* **2024**, *15*, 1507283, doi:10.3389/fimmu.2024.1507283.
22. Zonov, E.; Kochneva, G.; Yunusova, A.; Grazhdantseva, A.; Richter, V.; Ryabchikova, E. Features of the Antitumor Effect of Vaccinia Virus Lister Strain. *Viruses* **2016**, *8*, doi:10.3390/v8010020.
23. Yang, S.H.; Oh, T.K.; Kim, S.T. Increased anti-tumor effect by a combination of HSV thymidine kinase suicide gene therapy and interferon-gamma/GM-CSF cytokine gene therapy in CT26 tumor model. *J Korean Med Sci* **2005**, *20*, 932-937, doi:10.3346/jkms.2005.20.6.932.
24. Lemos de Matos, A.; Franco, L.S.; McFadden, G. Oncolytic Viruses and the Immune System: The Dynamic Duo. *Mol Ther Methods Clin Dev* **2020**, *17*, 349-358, doi:10.1016/j.omtm.2020.01.001.
25. Wu, Y.Y.; Sun, T.K.; Chen, M.S.; Munir, M.; Liu, H.J. Oncolytic viruses-modulated immunogenic cell death, apoptosis and autophagy linking to virotherapy and cancer immune response. *Front Cell Infect Microbiol* **2023**, *13*, 1142172, doi:10.3389/fcimb.2023.1142172.
26. Chen, L.; Zuo, M.; Zhou, Q.; Wang, Y. Oncolytic virotherapy in cancer treatment: challenges and optimization prospects. *Front Immunol* **2023**, *14*, 1308890, doi:10.3389/fimmu.2023.1308890.
27. Vaha-Koskela, M.; Hinkkanen, A. Tumor Restrictions to Oncolytic Virus. *Biomedicines* **2014**, *2*, 163-194, doi:10.3390/biomedicines2020163.
28. Xu, J.; Xia, Z.; Wang, S.; Xia, Q. Resistance to oncolytic virotherapy: Multidimensional mechanisms and therapeutic breakthroughs (Review). *Int J Mol Med* **2025**, *56*, doi:10.3892/ijmm.2025.5612.
29. Dagogo-Jack, I.; Shaw, A.T. Tumour heterogeneity and resistance to cancer therapies. *Nat Rev Clin Oncol* **2018**, *15*, 81-94, doi:10.1038/nrclinonc.2017.166.
30. Wu, B.; Zhang, B.; Li, B.; Wu, H.; Jiang, M. Cold and hot tumors: from molecular mechanisms to targeted therapy. *Signal Transduct Target Ther* **2024**, *9*, 274, doi:10.1038/s41392-024-01979-x.
31. Singh, D.D.; Haque, S.; Kim, Y.; Han, I.; Yadav, D.K. Remodeling of tumour microenvironment: strategies to overcome therapeutic resistance and innovate immunoengineering in triple-negative breast cancer. *Front Immunol* **2024**, *15*, 1455211, doi:10.3389/fimmu.2024.1455211.
32. Freeman, S.M.; Abboud, C.N.; Whartenby, K.A.; Packman, C.H.; Koeplin, D.S.; Moolten, F.L.; Abraham, G.N. The "bystander effect": tumor regression when a fraction of the tumor mass is genetically modified. *Cancer Res* **1993**, *53*, 5274-5283.

 doi:10.20944/preprints202605.0960.v1

33. Cao, G.; Ding, C.; Dai, J.; Qiu, X. Oncolytic virus and immunogenic cell death in cancer therapy. *Tumour Virus Res* **2025**, *20*, 200333, doi:10.1016/j.tvr.2025.200333.
34. Umegaki, S.; Shirota, H.; Kasahara, Y.; Iwasaki, T.; Ishioka, C. Distinct role of CD8 cells and CD4 cells in antitumor immunity triggered by cell apoptosis using a Herpes simplex virus thymidine kinase/ganciclovir system. *Cancer Sci* **2023**, *114*, 3076-3086, doi:10.1111/cas.15843.
35. Chen, R.; Kang, R.; Tang, D. The mechanism of HMGB1 secretion and release. *Exp Mol Med* **2022**, *54*, 91-102, doi:10.1038/s12276-022-00736-w.
36. Vultaggio-Poma, V.; Sarti, A.C.; Di Virgilio, F. Extracellular ATP: A Feasible Target for Cancer Therapy. *Cells* **2020**, *9*, doi:10.3390/cells9112496.
37. Guo, Y.; Luan, L.; Patil, N.K.; Sherwood, E.R. Immunobiology of the IL-15/IL-15Ralpha complex as an antitumor and antiviral agent. *Cytokine Growth Factor Rev* **2017**, *38*, 10-21, doi:10.1016/j.cytogfr.2017.08.002.
38. Van den Bergh, J.; Willemen, Y.; Lion, E.; Van Acker, H.; De Reu, H.; Anguille, S.; Goossens, H.; Berneman, Z.; Van Tendeloo, V.; Smits, E. Transpresentation of interleukin-15 by IL-15/IL-15Ralpha mRNA-engineered human dendritic cells boosts antitumoral natural killer cell activity. *Oncotarget* **2015**, *6*, 44123-44133, doi:10.18632/oncotarget.6536.
39. Kobayashi, H.; Dubois, S.; Sato, N.; Sabzevari, H.; Sakai, Y.; Waldmann, T.A.; Tagaya, Y. Role of trans-cellular IL-15 presentation in the activation of NK cell-mediated killing, which leads to enhanced tumor immunosurveillance. *Blood* **2005**, *105*, 721-727, doi:10.1182/blood-2003-12-4187.
40. Carter, A.B.; Tephly, L.A.; Hunninghake, G.W. The absence of activator protein 1-dependent gene expression in THP-1 macrophages stimulated with phorbol esters is due to lack of p38 mitogen-activated protein kinase activation. *J Biol Chem* **2001**, *276*, 33826-33832, doi:10.1074/jbc.M100209200.
41. Conlon, K.C.; Lugli, E.; Welles, H.C.; Rosenberg, S.A.; Fojo, A.T.; Morris, J.C.; Fleisher, T.A.; Dubois, S.P.; Perera, L.P.; Stewart, D.M.; et al. Redistribution, hyperproliferation, activation of natural killer cells and CD8 T cells, and cytokine production during first-in-human clinical trial of recombinant human interleukin-15 in patients with cancer. *J Clin Oncol* **2015**, *33*, 74-82, doi:10.1200/JCO.2014.57.3329.
42. Smith, R.L.; Traul, D.L.; Schaack, J.; Clayton, G.H.; Staley, K.J.; Wilcox, C.L. Characterization of promoter function and cell-type-specific expression from viral vectors in the nervous system. *J Virol* **2000**, *74*, 11254-11261, doi:10.1128/jvi.74.23.11254-11261.2000.
43. Verardi, P.H.; Jones, L.A.; Aziz, F.H.; Ahmad, S.; Yilma, T.D. Vaccinia virus vectors with an inactivated gamma interferon receptor homolog gene (B8R) are attenuated In vivo without a concomitant reduction in immunogenicity. *J Virol* **2001**, *75*, 11-18, doi:10.1128/JVI.75.1.11-18.2001.
44. Heichler, C.; Scheibe, K.; Schmied, A.; Geppert, C.I.; Schmid, B.; Wirtz, S.; Thoma, O.M.; Kramer, V.; Waldner, M.J.; Buttner, C.; et al. STAT3 activation through IL-6/IL-11 in cancer-associated fibroblasts promotes colorectal tumour development and correlates with poor prognosis. *Gut* **2020**, *69*, 1269-1282, doi:10.1136/gutjnl-2019-319200.
45. Wu, S.C.; Munger, K. Role and Clinical Utility of Cancer/Testis Antigens in Head and Neck Squamous Cell Carcinoma. *Cancers (Basel)* **2021**, *13*, doi:10.3390/cancers13225690.
46. Myskiw, C.; Arsenio, J.; van Bruggen, R.; Deschambault, Y.; Cao, J. Vaccinia virus E3 suppresses expression of diverse cytokines through inhibition of the PKR, NF-kappaB, and IRF3 pathways. *J Virol* **2009**, *83*, 6757-6768, doi:10.1128/JVI.02570-08.
47. Davies, M.V.; Chang, H.W.; Jacobs, B.L.; Kaufman, R.J. The E3L and K3L vaccinia virus gene products stimulate translation through inhibition of the double-stranded RNA-dependent protein kinase by different mechanisms. *J Virol* **1993**, *67*, 1688-1692, doi:10.1128/JVI.67.3.1688-1692.1993.
48. Allam, A.; Yakou, M.; Pang, L.; Ernst, M.; Huynh, J. Exploiting the STAT3 Nexus in Cancer-Associated Fibroblasts to Improve Cancer Therapy. *Front Immunol* **2021**, *12*, 767939, doi:10.3389/fimmu.2021.767939.
49. Ali, S.R.; Jordan, M.; Nagarajan, P.; Amit, M. Nerve Density and Neuronal Biomarkers in Cancer. *Cancers (Basel)* **2022**, *14*, doi:10.3390/cancers14194817.
50. Treitschke, S.; Weidele, K.; Varadarajan, A.R.; Feliciello, G.; Warfsmann, J.; Vorbeck, S.; Polzer, B.; Botteron, C.; Hoffmann, M.; Dechand, V.; et al. Ex vivo expansion of lung cancer-derived disseminated cancer cells from lymph nodes identifies cells associated with metastatic progression. *Int J Cancer* **2023**, *153*, 1854-1867, doi:10.1002/ijc.34658.

 doi:10.20944/preprints202605.0960.v1

51. Grisaru-Tal, S.; Dulberg, S.; Beck, L.; Zhang, C.; Itan, M.; Hediyeh-Zadeh, S.; Caldwell, J.; Rozenberg, P.; Dolitzky, A.; Avlas, S.; et al. Metastasis-Entrained Eosinophils Enhance Lymphocyte-Mediated Antitumor Immunity. *Cancer Res* **2021**, *81*, 5555-5571, doi:10.1158/0008-5472.CAN-21-0839.
52. Ghaffari, S.; Rezaei, N. Eosinophils in the tumor microenvironment: implications for cancer immunotherapy. *J Transl Med* **2023**, *21*, 551, doi:10.1186/s12967-023-04418-7.
53. Tosic, V.; Thomas, D.L.; Kranz, D.M.; Liu, J.; McFadden, G.; Shisler, J.L.; MacNeill, A.L.; Roy, E.J. Myxoma virus expressing a fusion protein of interleukin-15 (IL15) and IL15 receptor alpha has enhanced antitumor activity. *PLoS One* **2014**, *9*, e109801, doi:10.1371/journal.pone.0109801.
54. Stephenson, K.B.; Barra, N.G.; Davies, E.; Ashkar, A.A.; Lichty, B.D. Expressing human interleukin-15 from oncolytic vesicular stomatitis virus improves survival in a murine metastatic colon adenocarcinoma model through the enhancement of anti-tumor immunity. *Cancer Gene Ther* **2012**, *19*, 238-246, doi:10.1038/cgt.2011.81.
55. Nelson, A.; Gebremeskel, S.; Lichty, B.D.; Johnston, B. Natural killer T cell immunotherapy combined with IL-15-expressing oncolytic virotherapy and PD-1 blockade mediates pancreatic tumor regression. *Journal for immunotherapy of cancer* **2022**, *10*, doi:10.1136/jitc-2021-003923.
56. Zhang, Q.; Zhang, J.; Tian, Y.; Zhu, G.; Liu, S.; Liu, F. Efficacy of a novel double-controlled oncolytic adenovirus driven by the Ki67 core promoter and armed with IL-15 against glioblastoma cells. *Cell Biosci* **2020**, *10*, 124, doi:10.1186/s13578-020-00485-1.
57. Shakiba, Y.N., E.R.; Kochetkov, D.V.; Yusubalieva, G.M.; Vorobyev, P.O.; Chumakov, P.M.; Baklaushev, V.P.; Lipatova, A.V. Comparison of the oncolytic activity of recombinant vaccinia virus strains LIVP-RFP and MVA-RFP against solid tumors. *Bulletin of RSMU* **2023**, 4-12, doi:10.24075/vrgmu.2023.010.
58. Sambrook, J.; Russell, D.W. Purification of nucleic acids by extraction with phenol:chloroform. *CSH Protoc* **2006**, *2006*, doi:10.1101/pdb.prot4455.
59. Shakiba, Y.; Vorobyev, P.O.; Naumenko, V.A.; Kochetkov, D.V.; Zajtseva, K.V.; Valikhov, M.P.; Yusubalieva, G.M.; Gumennaya, Y.D.; Emelyanov, E.A.; Semkina, A.S.; et al. Oncolytic Efficacy of a Recombinant Vaccinia Virus Strain Expressing Bacterial Flagellin in Solid Tumor Models. *Viruses* **2023**, *15*, doi:10.3390/v15040828.
60. Comparative efficiency of accessible transfection methods in model cell lines for biotechnological applications. *Bulletin of RSMU* **2022**, doi:10.24075/brsmu.2022.031.
61. Cotter, C.A.; Earl, P.L.; Wyatt, L.S.; Moss, B. Preparation of Cell Cultures and Vaccinia Virus Stocks. *Curr Protoc Protein Sci* **2017**, *89*, 5 12 11-15 12 18, doi:10.1002/cpps.34.
62. Schmittgen, T.D.; Livak, K.J. Analyzing real-time PCR data by the comparative C(T) method. *Nat Protoc* **2008**, *3*, 1101-1108, doi:10.1038/nprot.2008.73.
63. Feldman, A.T.; Wolfe, D. Tissue processing and hematoxylin and eosin staining. *Methods Mol Biol* **2014**, *1180*, 31-43, doi:10.1007/978-1-4939-1050-2_3.